



The effect of thermal frequency and current amplitude on weldability, microstructural evolution and mechanical properties of AA7075 alloy joint in DP-GMAW process

Behnam Soltani¹ · Amirreza Farnia¹ · S. H. Mousavi Anijdan¹

Received: 21 August 2020 / Accepted: 24 January 2021 / Published online: 5 February 2021
© The Author(s), under exclusive licence to Springer-Verlag London Ltd. part of Springer Nature 2021

Abstract

In this study, the effect of dual-pulsed gas metal arc welding (DP-GMAW) parameters such as thermal frequency and current amplitude on weldability, microstructural evolution, and mechanical properties of AA7075 alloy joint was investigated. ER53356 filler metal was employed to make AA7075 alloy joints. Thermal frequency in three levels of 1, 2, and 3 Hz was used during the welding process. And current amplitudes of 9, 27, and 45 A were used in three levels as well. After the DP-GMAW process, the welded samples were first checked visually, by a liquid penetrant method, to make sure of their welding soundness. No surface defect or crack was observed. An optical microscope (OM) and a scanning electron microscope (SEM) equipped with energy-dispersive spectroscopy (EDS) were used for microstructural analyses. The hardness of the base metal (BM) and different areas of the welded parts was measured by a microhardness testing method. Results showed that no visual defects were visible on the surface of the joints made under different PD-GMAW variables. As well, microstructural analyses showed that increasing the thermal frequency and current amplitude not only reduced the grain size of the weld metal (WM) and the heat-affected zone (HAZ) but also increased the hardness of these regions. The most refined structure was obtained by employing 2 Hz as frequency and 45 A as current amplitude. The average grain size under these conditions was 71 μm and 52 μm , respectively. It was also observed that increasing the current amplitude had the highest impact in reducing the grain size of the WM. The hardness of the WM and the HAZ, under the optimum frequency, was 91 HVN and 153 HVN, respectively. These values were 85 HVN and 38 HVN under the optimum current amplitude. Moreover, hardness was increased in the HAZ compared with the base metal in all welding conditions. Increasing the thermal frequency not only decreased the distance between the ripples but also increased the number of peak waves created in the fusion line. This was particularly the case in the longitudinal section of the weld and reduced the distance between these waves. On the other hand, increasing the frequency and current amplitude has led to the reduction of porosity in the WM. Finally, increasing the frequency from 1 to 3 Hz led to a 33% reduction in the porosity of the WM. This is while 66% reduction of porosity in the WM was obtained by increasing the current amplitude from 9 to 45 A.

Keywords AA7075 alloy · DP-GMAW · Thermal frequency · Current amplitude · Hardness · Porosity

1 Introduction

In advanced materials, welding techniques, or in other words, the jointing processes to expand the working application are of critical importance [1]. Special cares are needed control the chemical composition, microstructure, and mechanical

performance of the joint for the advanced materials [2]. Of the methods used for such a joint, arc welding techniques are very attractive to study the microstructure and mechanical properties of these materials [3].

AA7075, as a strategic alloy, has been used in some critical sectors such as aerospace, and recently in automotive, industries [4]. It has been reported [5] that of the unique characteristics of AA7075 alloy are the high ratio of strength to weight, high strength, excellent toughness, and corrosion resistance. One of the fundamental limitations of this alloy is its poor weldability, especially by arc welding processes. In other words, welding of this alloy by arc welding processes has some serious metallurgical problems in the weldment.

✉ Amirreza Farnia
a.farnia@srbiau.ac.ir

¹ Department of Materials Engineering, Science and Research Branch, Islamic Azad University, Tehran, Iran

Defects such as porosity of the weld metal (WM), the presence of cracks, and rapid reduction of strength in this region are quite common. Solidification cracks or hot cracking is one of the fundamental problems in the welding of age hardening alloy [6, 7].

Besides, swift reduction of the mechanical properties of the weld zone, compared with that of the base metal, is of critical welding predicament for this alloy [8]. Mishra and Ma [9] elucidated the use of friction stir welding processing for the jointing of this alloy. Moreover, Squillace et al. [10] described that the mentioned factors make conventional melt welding processes of the AA7075 aluminum alloy parts relatively ineffective. Therefore, employing new welding techniques for the special alloys joint to avoid metallurgical defects is of the prime focus of researchers [11].

Of the problem encountered in the welding of 7000 series aluminum alloy is the occurrence of solidification cracks [7]. In that sense, the presence of copper in the composition of these alloys, particularly if more than 0.8 wt% Cu is added, leads to a wide melting range and reduction of solidus temperature and consequently increases sensitivity to crack in the joint region under the influence of melting processes. Based on these, two distinguished regions can be formed during the solidification process: an area enriched with copper, and a region depleted of copper. The first region solidifies faster/sooner, and the second region, due to lower melting point, solidifies slower/late. Taking into account the difference in the solidification rate at the interface of solid and liquid, the probability of the occurrence of shrinkage stress resulting from the infilling of the weld metal increases [12]. As well, the presence of magnesium and zinc leads to liquid evaporation of the melt region. This effect is due to their low vaporization temperature and high vaporization pressure. Hazler et al. [13] showed that sensitivity to the solidification crack severely increases under the condition where 5.5 wt% and 1.5 wt% of Zn and Cu, respectively, exist in the base metal.

Conventional GMAW process and continuous cooling GMAW (CCGMAW) process were widely used to join aluminum alloys. The type of welding current is of the main variables in these processes. Moreover, continuous current and pulsed current are the two fundamental variables in the GMAW process. Compared with the pulsed current, the continuous current would lead to a sensible reduction of properties in the joint. This is while using pulsed current not only improves the solidification structure of the weld metal by grain refinement mechanism but also enhances the mechanical properties of the joint [14, 15].

Yi et al. [16] indicated that among the welding processes, dual-pulse GMAW (DP-GMAW) process, as another type of the pulse current, has gained a widespread application in different industries for joining aluminum alloys. Da Silva and Scotti [17] showed that, compared with the P-GMAW process, the DP-GMAW technique has some advantages such as reduction

of the WM porosity and improvement in crack sensitivity. Also, among the welding variables, thermal frequency and current amplitude are the main effective parameters in the DP-GMAW process. They have a significant influence on the properties of the weldment. Thermal frequency, as the most influential variable of the DP-GMAW process, substantially changes the arc force and the heat input of the process. It can control the amount of the latter parameter. As well, Liu et al. [18] presented that an improvement in the visual appearance of the welded region, due to the formation of very fine and continuous structure, is another effect of the thermal frequency. Alternatively, current amplitude, as another variable of the DP-GMAW process, is influenced by the average current of the pulse thermal phase (I_T) and the average current of the field phase (I_S). For example, Wang et al. [19] reported that its value is equal to half of the average current phase of the initial pulse minus the average current of the field phase. This variable controls the average cooling rate under the fixed heat input.

Various studies were performed to assess the effect of pulse current parameters on the properties of the weldment. Based on the findings of Mendes da Silva and Scotti [20], DP-GMAW not only reduces the porosity of the WM but also lowers the tendency for the solidification crack. Grain refinement in the WM, under the DP-GMAW technique, is one of the mechanisms that was introduced regarding the improvement or prevention of the occurrence of solidification cracking. A refined grain structure generates lower tensile strain during the solidification contraction due to its higher percentage of grain boundary areas in a unit volume [17]. On the other hand, the refined grain structure can better adapt itself with the contraction strains. Another view is that a change in the direction of the grains in a refined structure stops the growth of the solidification cracks [15]. Therefore, as the growth path of the cracks is continually changing, the cracks cannot continue their growth.

In another study, Yao et al. [21] compared the two processes of DP-GMAW and P-GMAW. They reported an improvement of metallurgical/mechanical properties of the weldment produced by DP-GMAW process. Higher hardness and better tensile properties of the weldment in aluminum alloys were among the benefits of this welding technique. Also, based on the findings of Nakata et al. [22], in employing DP-GMAW process, the rate of corrosion crack of the WM of A7N01 aluminum alloy was reduced. As well, Yamamoto et al. [23] investigated the grain size reduction of the WM under the influence of thermal frequency. Their findings showed that the average grain size of the WM was reduced by increasing the thermal frequency of the process.

Current amplitude, as another important parameter of the DP-GMAW process, is highly influential for the properties of the weldment. In a study conducted on the effect of current amplitude, it has been shown that increasing the value of this parameter reduces the grain size of the WM. Furthermore,

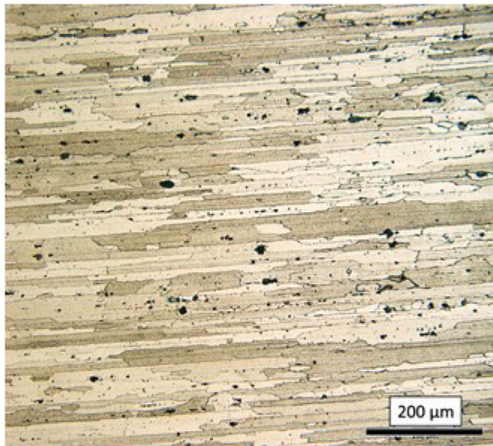


Fig. 1 The microstructure of the base metal; AA7075 alloy

microstructural refinement of the WM was achieved under the influence of higher current amplitude when other welding parameters were kept constant [19].

In addition, Wang and Xue [24] illustrated that the reduction of the heat input, and also increasing the shrinkage, and the expansion of the weld pool are of the consequences of increasing the current amplitude. In terms of the effect of the current amplitude on the amount of porosity in the weldment of AA7075 alloy during the dual-pulsed arc welding process weldment of AA7075 alloy, no in-depth analysis can be found in the literature.

Porosity is one of the most known defects when fusion-based methods are used for aluminum alloy [25]. This defect can substantially deteriorate the mechanical properties of the weldment. Extensive researches were done to eliminate or reduce this defect and to define the reasoning for its occurrence. The strategies used in that respect included shielding gas optimization [26], using two-beam technology [27], using a modulated laser power system [28], using an oscillating laser beam [29, 30], and the generation of Lorentz forces in the weld pool [31].

Although numerous studies were conducted on the effect of process parameters of the DP-GMAW process on the properties of the weldment of various aluminum alloys, no analysis was performed to explain the impact of these process parameters on the welding characteristics of AA7075 alloy. As well, the effect of dual-pulsed arc welding technique parameters on the width of the columnar zone is another point that has not been paid attention to date and is the subject of this study. It is essential to mention that the occurrence of weld metal porosity

Table 2 Standard mechanical properties of the AA7075 alloy in T6 aged condition [32]

Elastic modulus (GPa)	EL (%)	Yield strength (MPa)	Ultimate tensile strength (MPa)	Hardness (VHN)
71.7	11	572	503	175

is one of the problems encountered in pulsed process welding. To the best of the authors' knowledge, this issue has not been explored in detail and is, therefore, one of the main focuses of the current study. Thus, this study aims to examine the effect of DP-GMAW process parameters, such as thermal frequency and current amplitude, on some the properties of AA7075 alloy such as weldability, microstructural evolution, and hardness. In a sense, this study intends to achieve optimum property combinations by changing the main parameters of the DP-GMAW process.

2 Materials and experimental procedure

The base metal used for the DP-GMAW welding process was an AA7075 aluminum alloy. Figure 1 shows the microstructure of the base metal used in this study.

An ER5356 filler metal with the characteristic of AlMg₅ and with the diameter of 0.5 mm was used for the welding process. The chemical compositions of the base metal and the filler metal are given in Table 1. Table 2 also gives the standard mechanical properties of the AA7075 alloy in the T6 aged condition.

Samples were cut to the dimensions of 150*100*5 mm. A single V joint design with the approximate bevel angle of 36° was made on the samples. The shape was created by a milling machine with a diamond blade. To complete the preparation step, and to make a uniform surface, the joints were further refined manually by a grater. Before the welding process, all joints were first degreased and then cleaned by acetone solution. And, a final oxide removal was applied as well. A schematic of the joint is shown in Fig. 2.

The welding process was performed by a DP-GMAW machine, with the characteristic of DIGI MIG-502, equipped with a cooling system. Argon gas with the purity of 99.99 was used as the protecting atmosphere. The welding parameters employed are given in Table 3. Also, Fig. 3 shows a

Table 1 Chemical compositions of AA7075 alloy and ER5356 filler metal

	Zn	Mg	Cu	Mn	Fe	Si	Cr	Ti	Al
AA7075	6.21	2.17	1.66	0.07	0.194	0.08	0.191	0.0196	Balance
ER 5356	0.04	4.86	0.01	0.15	0.12	0.06	0.06	0.08	Balance

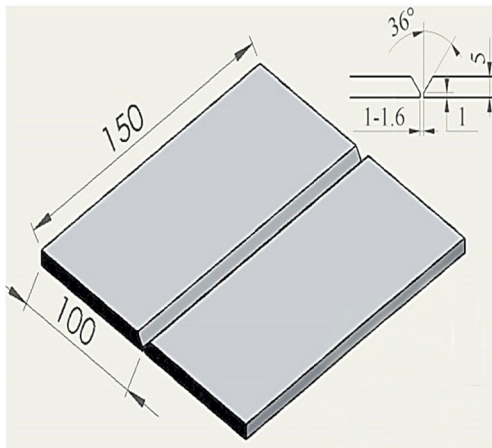


Fig. 2 A schematic of the joint design made for the DP-GMAW process

schematic of the welding wave and the parameters of the DP-GMAW process used for different samples.

As well, a back purging gas was continuously used, similar to the configuration shown in Fig. 4, with the flow of 20 lit/min to protect the back of the piece against oxidation.

The microstructures of the welded joints were studied by using an optical microscope (OM), a field emission scanning electron microscope (FE-SEM) equipped with energy-dispersive spectroscopy (EDS), and with a detector of EDAX EDS Silicon Drift made in the USA. All grains were counted in each OM micrograph and sorted based on the average diameter of the grains. The values obtained were reported in the form of histograms as true values. As well, the amount of porosity in every weld was measured based on the counting of the number of porosities in the transfer section of the weld.

Microhardness tests were done on the samples that were analyzed for microstructural studies. For this purpose, The Vickers microhardness measurements were performed by using a Shimadzu microhardness apparatus. A 50-gr N load

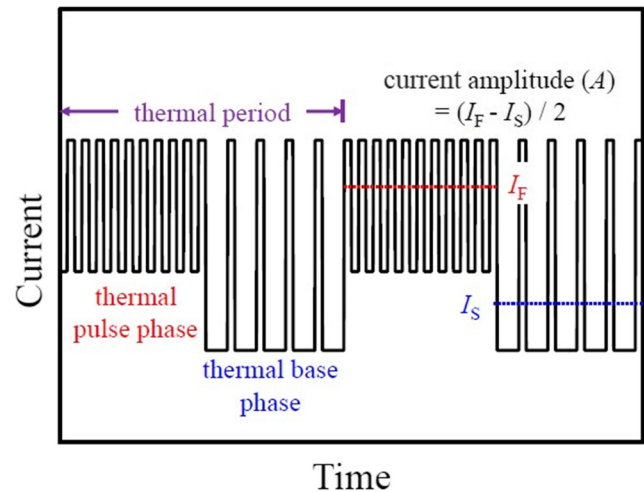


Fig. 3 The shape of the wave and the variables of the DP-GMAW process [20]

was applied for 10 s on the WM, HAZ, and the base metal. The average of five measurements was reported for the hardness tests to make sure of the repeatability of the tests.

3 Results and discussion

3.1 Visual feature of the weld

Figure 5 shows the feature of the WM made under the influence of various thermal frequencies. As can be seen in this figure, the WMs do not display any defects. The visual feature of the welds was transformed under the influence of the thermal frequency in a way that reduction in the frequency has led to an increase in the distance between the weld ripples. This was more pronounced as the thermal frequency decreased from 3 to 1 Hz. Moreover, it is observed in analyzing the macrostructure of the longitudinal section of the WM that the thermal frequency changes lead to the interface variation

Table 3 Welding parameters of the DP-GMAW process employed to join AA7075 alloy

Parameter	Sample 1	Sample 2	Sample 3	Sample 4	Sample 5
Welding current mode	DP-GMAW	DP-GMAW	DP-GMAW	DP-GMAW	DP-GMAW
Thermal frequency (Hz)	1	2	3	1	1
Current amplitude (A)	9	9	9	27	45
Voltage (V)	17.9	17.9	17.9	17.9	17.9
Average current (A)	90	90	90	90	90
First phase time (S)	0.5	0.5	0.5	0.5	0.5
Second phase time (S)	0.5	0.5	0.5	0.5	0.5
Average current of the first phase (A)	99	99	99	117	135
Average current of the second phase (A)	81	81	81	63	45
Welding speed ($\text{mm}\cdot\text{s}^{-1}$)	4	4	4	4	4
Contact tube to work distance (mm)	8–10	8–10	8–10	8–10	8–10

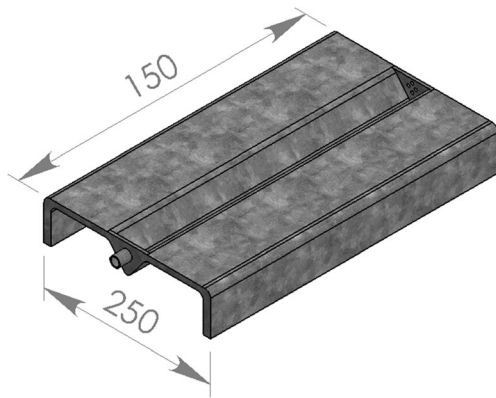


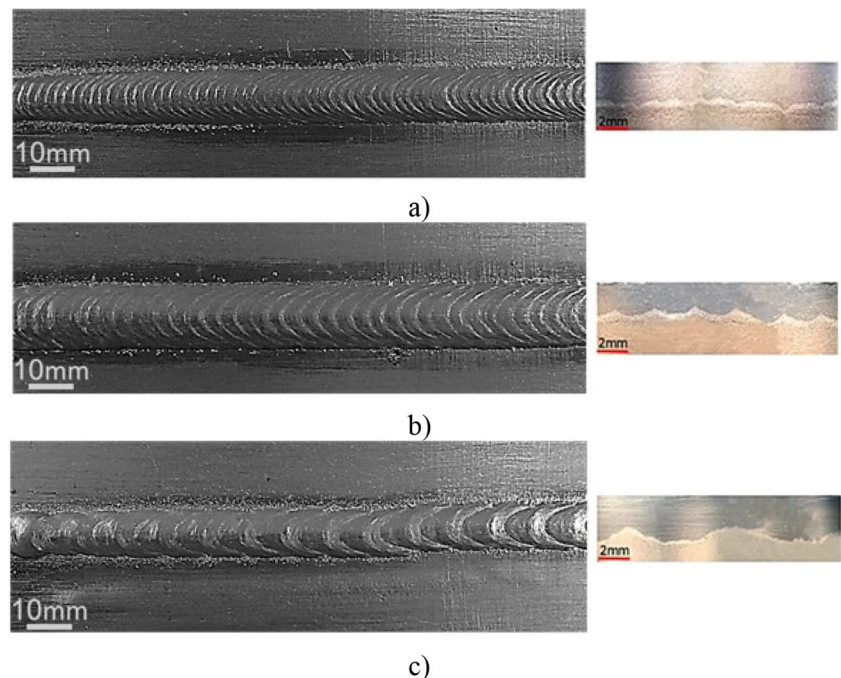
Fig. 4 The protection unit to apply back purging gas

of the weld metal and the base metal as well. This interface is called the fusion line. Under such circumstances, the weldment has become wavy in a way that with increasing the frequency, in addition to an increase in the number of waves (peaks), the distance between these peaks is reduced. As the welding current in the first phase (thermal pulse phase or TP) is way higher than the second phase (thermal base phase or TB), the highest diffusion depth of the WM occurred under this condition. On the other hand, the highest peak was seen in the thermal base phase. In Fig. 5, the average values for the distance between the peaks and the valleys were 3.3, 1.3, and 0.5 μm for the frequencies of 1, 2, and 3 Hz, respectively.

3.2 Microstructural analysis

The microstructures of the weldment under different thermal frequencies are shown in Fig. 6.

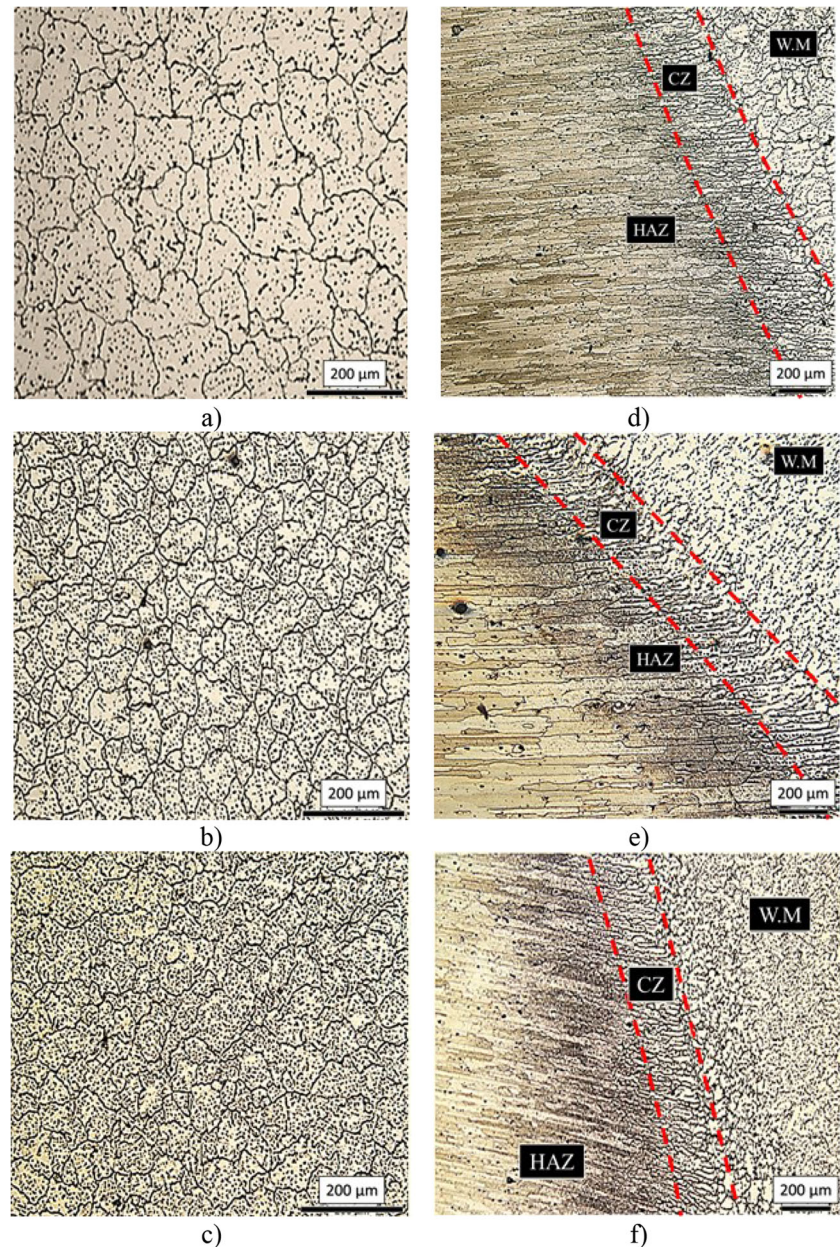
Fig. 5 Visual feature of the WM and the longitudinal section of the weldment under different thermal frequencies. **a** 3 Hz. **b** 2 Hz. **c** 1 Hz



It is known that the metal undergoes rapid solidification by increasing the thermal frequency, which in turn leads to the occurrence of surface nucleation, i.e., heterogeneous nucleation. This is due to a sudden and fast decrease of the heat input in a very short period of time. Besides, the reduction of the temperature of the melt pool aids the nucleated embryo to remain in the pool [33]. Therefore, the preferred locations of the nucleation get more directionality with increasing the frequency. This would lead to further grain refinement, as observed in Fig. 6a, b, and c. Another important point to consider in relation with increasing the frequency of the melt pool is the fact that the weld pool is alternatively agitated under the influence of frequency. As a result, this agitation of the melt pool increases with increasing the frequency. This effect leads to a substantial heat transfer from the melt pool. This phenomenon results in a higher solidification rate under the condition of higher frequency. It also results in better control of grain growth [34].

Goyal et al. [35] reported, in their investigation of the influence of pulse parameters on the characteristics of bead-on-plate weld deposits of aluminum and its alloys, that as the electric arc is the cause of heat creation, the behavior of the arc under the condition of increasing frequency will subsequently oscillate. Also, Engler and Hirsch [36] showed that such a phenomenon leads to better grain refinement in addition to the removal of the bubbles from the WM, hence for an improvement of the quality of the weldment. As well, when the intrinsic oscillation frequency of the weld pool and the thermal frequency of the DP-GMAW reach an equilibrium state, the resonance of the weld pool will be the highest which leads to the best grain refinement condition. Based on the

Fig. 6 Microstructures of the weldment. **a** WM-1Hz. **b** WM-2Hz. **c** WM-3Hz. **d** Interface-1Hz. **e** Interface-2Hz. **f** Interface-3Hz



observations of this study, 2-Hz frequency provides the highest amount of grain refinement in the structure among the cases studied. This is due to the closeness of the intrinsic oscillation frequency of the weld pool and the thermal frequency of the process as such. Jin et al. [37] observed that in this thermal frequency level, the WM is in equilibrium with the intrinsic oscillation frequency of the weld pool. Figure 7 demonstrates the grain size histogram under various thermal frequencies.

The partially melted zone (PMZ) is among the regions that have undergone transformation under the influence of different parameters of the pulse current. This region shows a coarse columnar structure and is located in between the WM and the

HAZ. Fig. 6d, e, and f show the interface of the WM, the HAZ, and the PMZ under the influence of thermal frequency. As can be observed in these figures, increasing the frequency from 1 to 3 Hz significantly reduced the length of the columnar region in the interface of the melting region. In other words, increasing the frequency prevented the spread of the columnar region. Consequently, it led to the narrowness of the columnar region under such a circumstance. The total area of the columnar zone under the frequencies of 1 Hz, 2 Hz, and 3 Hz were 267 μm , 202 μm , and 181 μm , respectively.

It is also known that the amount of heat input is the main factor in changing the HAZ area and causes microstructural changes in this region [38]. Therefore, no discernible

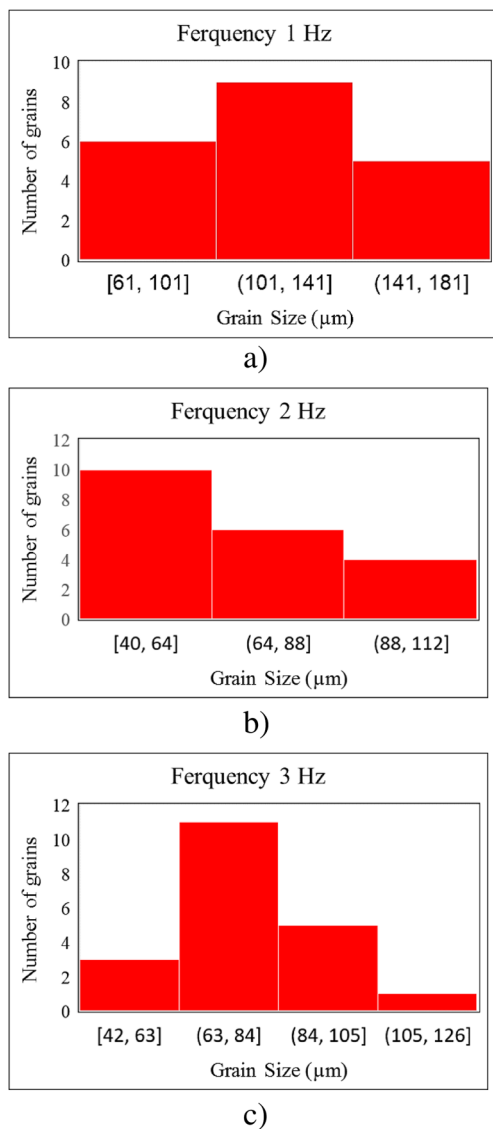


Fig. 7 Variation of the average grain size of the WM under different thermal frequencies. **a** 1 Hz. **b** 2 Hz. **c** 3 Hz

difference was observed in the HAZ region. The average grain size of this region under the frequency of 1 Hz, 2 Hz, and 3 Hz were 59 μm , 54 μm , and 55 μm , respectively. In a sense, the microstructural changes occurring in this region were not significant. Wang et al. [39], in their study of the effect of thermal frequency on AA6061 aluminum alloy, illustrated that this is, in fact, due to the negligible impact of the thermal frequency on the heat input.

Figure 8 shows the microstructure of the weldment under the influence of the current amplitude. It is observed that the grain size of the WM was reduced by increasing the current amplitude. This can be deduced from the comparison of Fig. 8a, b, and c. In fact, the current amplitude is affected by the average current of the thermal pulse phase (I_F) and the average current of the thermal base phase (I_S). Since the current is high, the thermal pulse phase (T_P) would show a higher arc force.

On the other hand, Rokhlin and Guu [40], in their study of the arc force, pool depression, and weld penetration, reported that, due to the current being low, the thermal base phase (T_B) has the lowest amount of arc energy due to the low current. Therefore, the thermal pulse phase (T_P) has a much higher impact function compared with the T_B phase. Additionally, under this condition, the surface of the melt pool periodically experiences oscillations. As a result, the agitation created by these oscillations causes a substantial amount of heat transfer out of the melt pool. This phenomenon increases with increasing the current amplitude.

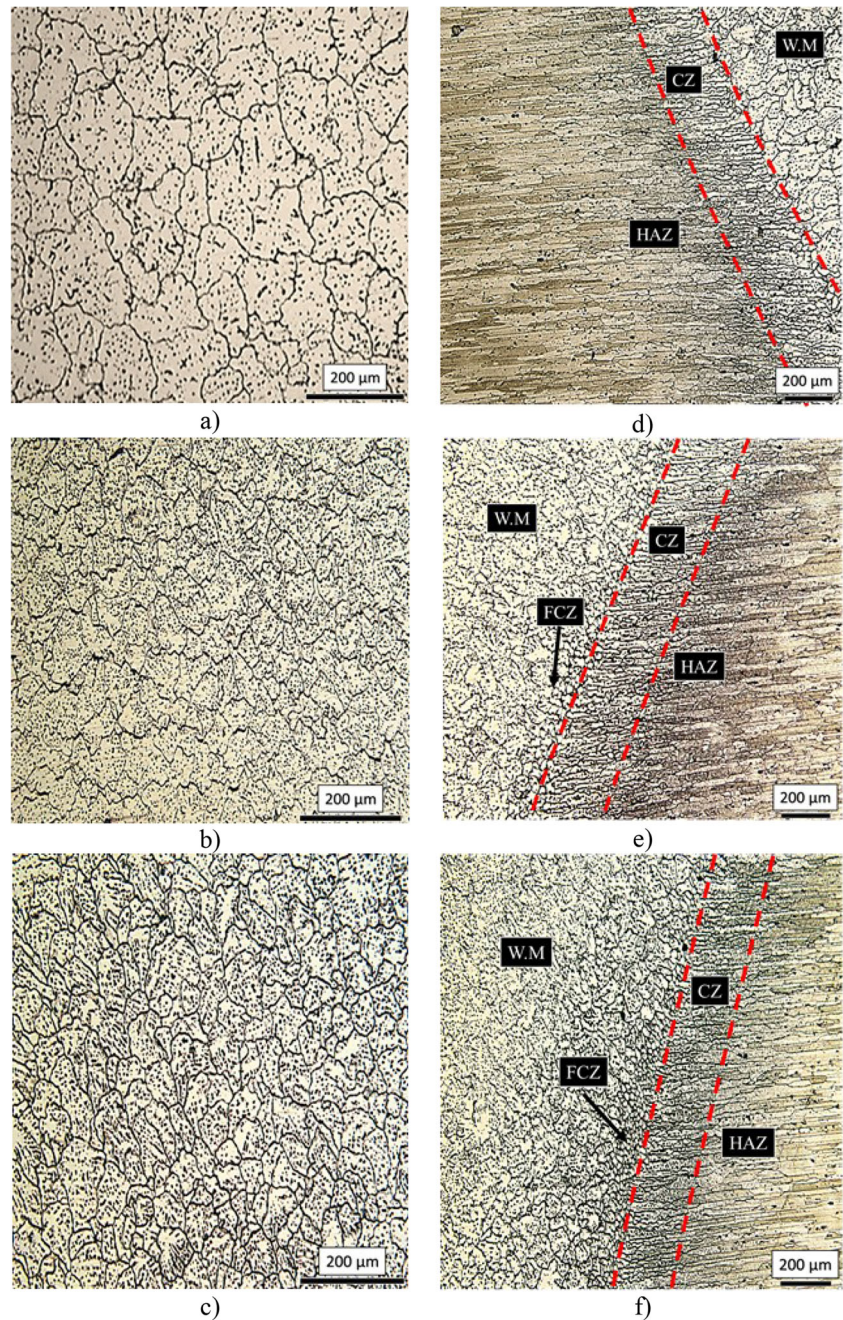
Consequently, this phenomenon affects the solidification process and delays grain growth. Wang et al. [39] introduced these reactions as scouring and shearing. These phenomena lead to the breakdown of the grains. And the broken grains act as nucleation sites the formation of new grains.

Another aspect of this phenomenon is the increase in the solidified area due to the rise in the current amplitude, where this parameter remarkably increases the solidification rate. In fact, the current amplitude controls the cooling rate under constant heat input. Wang [41] reported that increasing the cooling rate reduces the solidification time, due to its effect on increasing the average cooling rate, and, at the same time, stops the grain growth. The results of this research showed that the best condition was obtained for the current amplitude of 45 A in a way that it reduced the grain size for 57% compared with the current amplitude of 9 A. The histograms of Fig. 9 show the grain size variation at different current amplitudes.

The columnar PMZ microstructure was also affected by the changes in current amplitude. Decreasing the area of the columnar zone was another consequence of increasing the current amplitude. The areas of the columnar zone under the current amplitudes of 9 A, 27 A, and 45 A were 267 μm , 250 μm , and 149 μm , respectively. Moreover, the welded samples under the current amplitudes of 27 A and 45 A contained fined cellular zone (FCZ). They are shown by arrows in Fig. 8e and f. It is important to mention that this change in the microstructure was more severe under the current amplitude of 45 A.

Based on the microstructural assessment, no solidification cracking was observed. Such a crack is a common problem in the arc welding process of this alloy, as was observed. In terms of the improvement mechanisms or prevention for the occurrence of solidification cracks, a substantial reduction of grain size in the weldment was proposed as one of the influential factors in the DP-GMAW technique. A refined grain structure produces lower tensile strains during the solidification shrinkage as a result of a higher amount of grain boundary area per unit volume [42]. In other words, a refined grain structure can better withstand contraction strains. Another view proposed by Wang et al. [19] deals with the changing directionality of

Fig. 8 Microstructural changes in the weldment. **a** WM-9A. **b** WM-27A. **c** WM-45A. **d** Interface-9 A. **e** Interface 27 A. **f** Interface 45A



the grains in the refined structure, which prevents the growth of the solidification cracks. Therefore, cracks cannot continue their propagation due to the constant change in their growth direction. A significant difference between the current findings and the literature is the substantial reduction in the grain size of the weldment under the DP-GMAW process compared with the techniques such as continuous current (CC)-GMAW and pulsed (P)-GMAW. This can be particularly noticed by comparing the current results with the findings of Balasubramanian et al. [14, 15].

3.3 SEM results and EDS analysis

Figure 10 shows the SEM micrographs of the microstructure of the joint region. The microstructure of the WM consists of a casting structure together with the eutectic structure distributed in the grain boundary areas. Also, the HAZ has kept its rolling structure. Evidently, the precipitates are well-distributed in the grain boundary areas and within the matrix as such. As well, the distribution of the precipitates in the microstructure of the BM is observed in this figure.

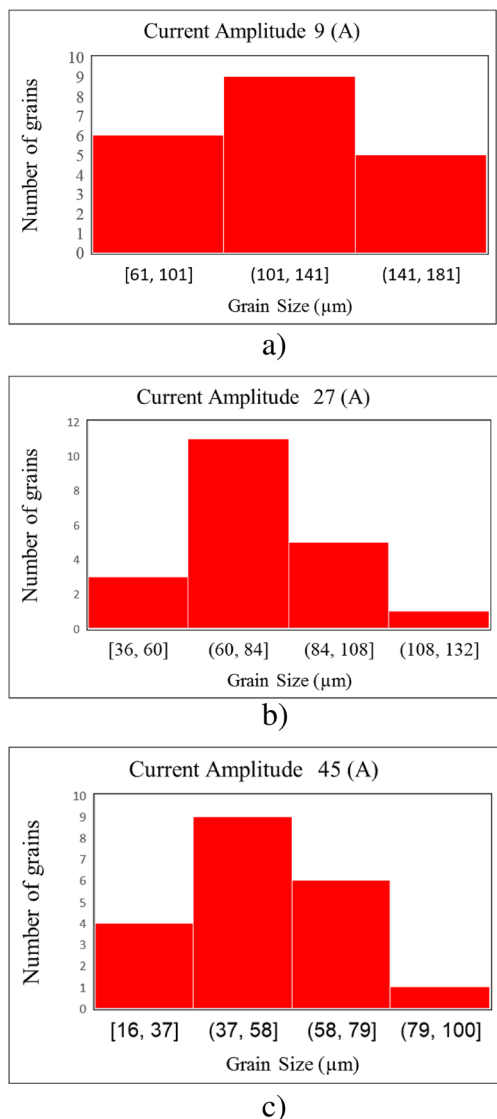


Fig. 9 Variation of the average grain size of the WM at different current amplitudes. a 9 A. b 27 A. c 45 A

EDS analyses were performed for the three regions of BM, HAZ, and the WM generated from ER5356. Figure 11 shows the results of these EDS analyses for the BM. It is important to mention that the low value of Si, shown in the figure, is unreliable.

As $MgZn_2$ (M phase), $CuAl_2$, and Al_7Cu_2Fe precipitates are the three primary precipitates in strengthening the AA7075 alloy, these precipitates were widely seen in the microstructure. As well, Mg_2Si precipitates are quite common in this type of alloy. Moreover, the black areas, that is extensively distributed in the structure, are indicators of the presence of Zn-, Si-, and Mg-enriched precipitates. They confirm the presence of $MgZn_2$ and Mg_2Si in the structure. Moreover, the brighter areas in the microstructure, which are quantitatively lower in the structure, are related to $CuAl_2$, Al_7Cu_2Fe , and possibly $Al_2Mg_3Zn_3$ (T phase) precipitates. This latest precipitate is mostly distributed in the metal matrix. Indeed, the highest amount of Cu to form $CuAl_2$ precipitates was 1.6wt%, whereas higher amounts of Zn and Mg are present in the structure to form $MgZn_2$ precipitates. As well, at point A, the weight percent of Al and Cu elements is substantially higher than other alloying elements, hence for the likelihood of the presence of $CuAl_2$ and Al_7Cu_2Fe precipitates. Therefore, this structure is indicative of the existence of Cu- and Zn-enriched precipitates, i.e., $MgZn_2$ enriched with Cu.

Additionally, at point B, in addition to Al, significant amounts of Si, Zn, and Mg were seen which is suggestive of the presence of Al-Zn-Mg-Si-enriched precipitates, i.e., α type precipitates. It is important to mention that the transmission electron microscope (TEM) analysis is necessary to define the phase composition and the type of precipitates precisely. Such analysis was beyond the scope of this study as the current effort was focused on understanding the effect of welding parameters.

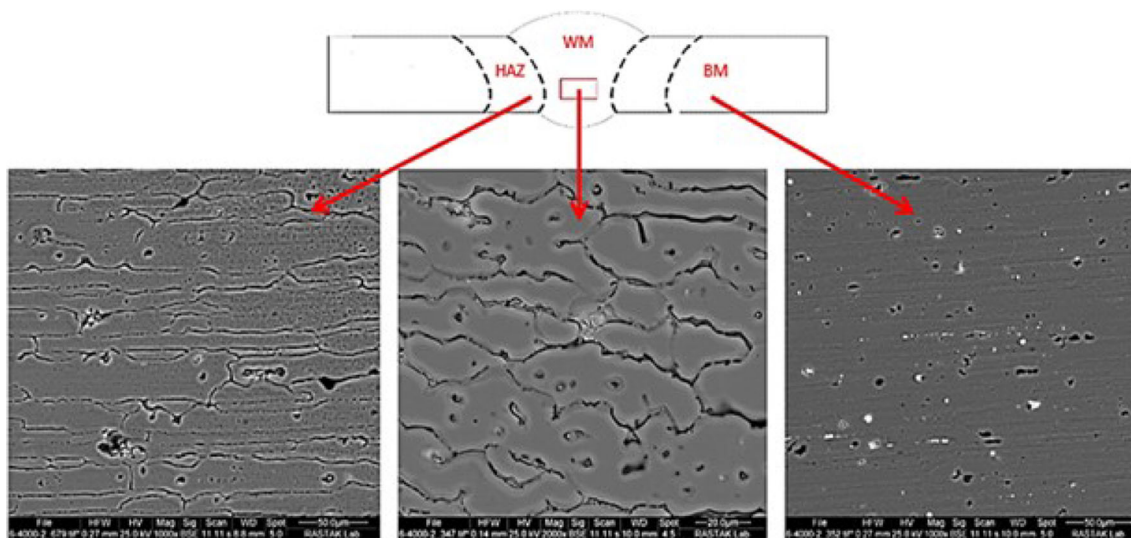


Fig. 10 SEM micrographs of the microstructure of the joint region

Fig. 11 SEM micrograph and EDS analyses of the BM in T6 heat-treated condition for the AA7075 alloy. **a** SEM micrograph of the BM. **b** EDS analysis of point A. **c** EDS analysis of point B

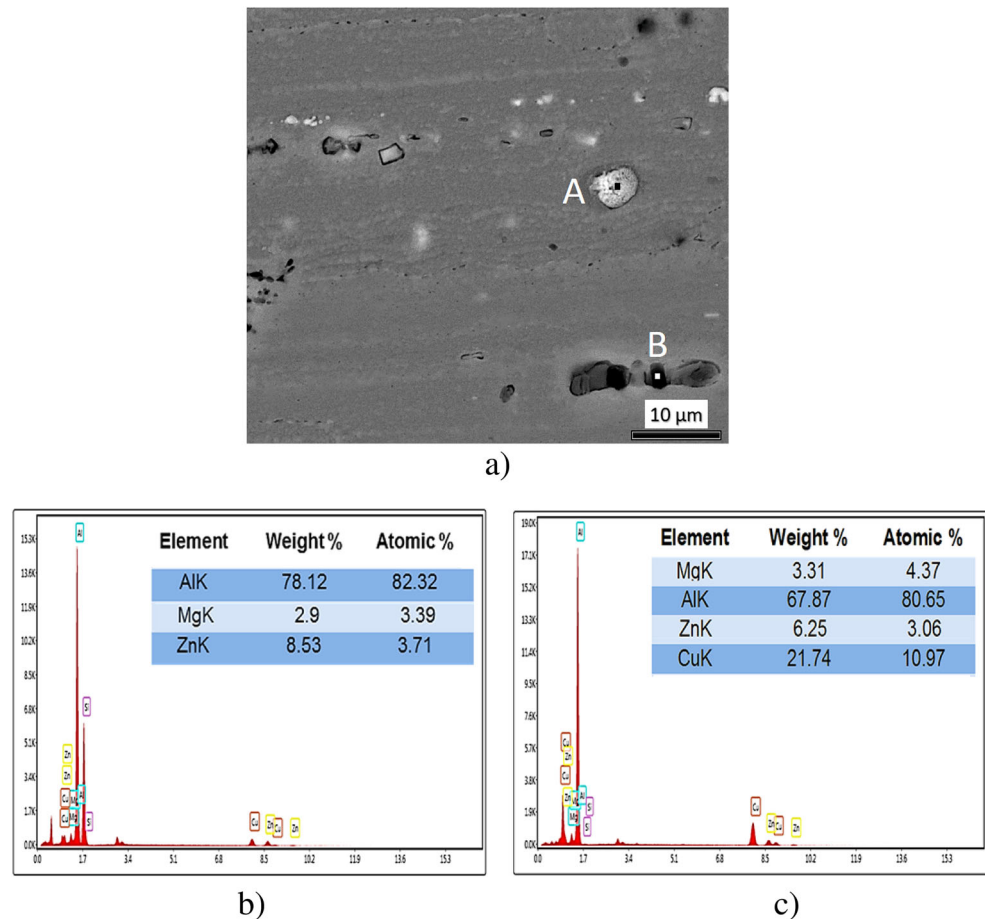


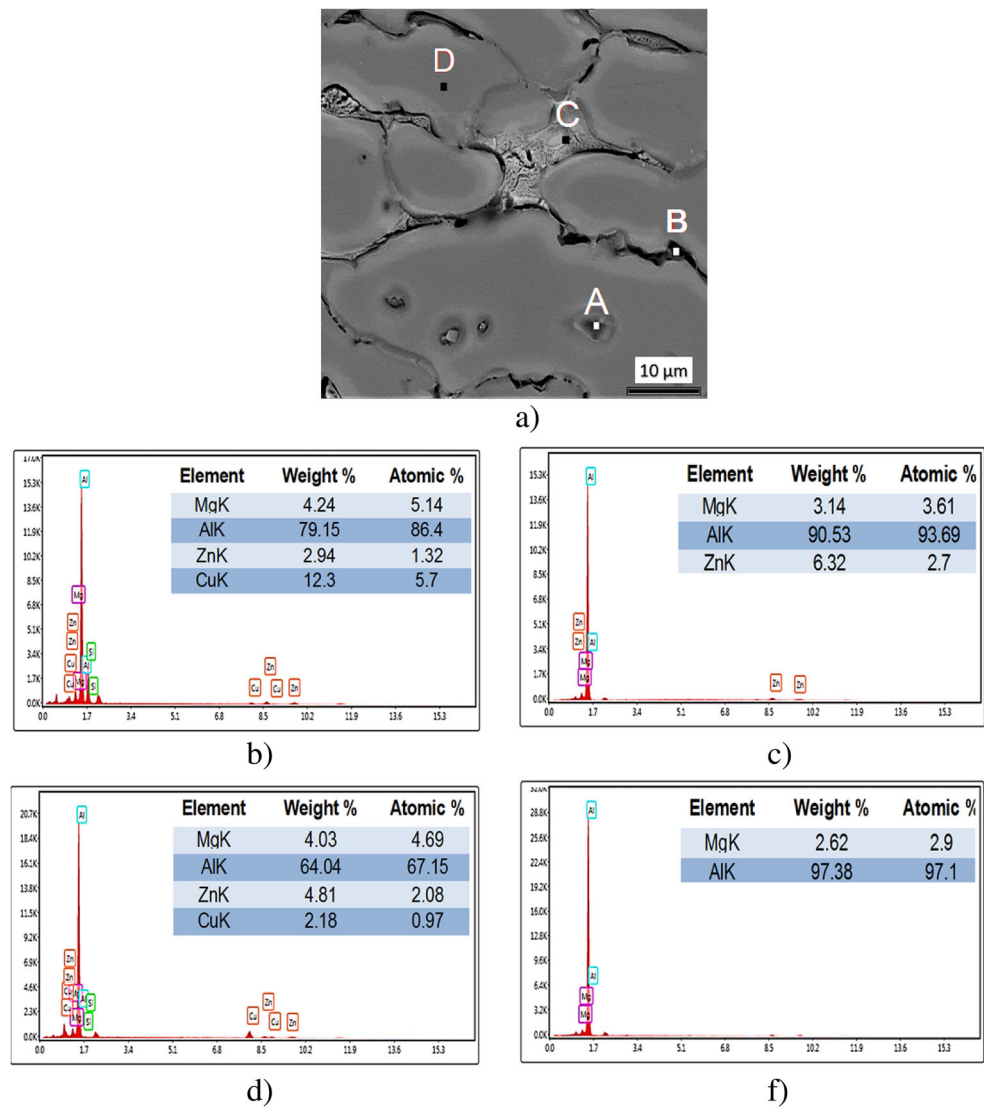
Figure 12 shows the EDS analysis of the WM. It is important to mention that the low value of Si, shown in the figure, is unreliable. At point A, after Al, Cu, and Mg show highest amounts with 12.3 wt% and 4.24 wt%, respectively. This points to the presence of $Al_2Cu(Mg)$ type precipitates in the microstructure. The amount of Si at this point is relatively low. While in black point such as B on the grain boundaries, that has about 90.53wt% Al, the amounts of Zn and Mg are 6.32 wt% and 3.14 wt% respectively. This is indicative of the presence of Zn- and Mg-rich precipitates, i.e., strengthening precipitates. No amount of Cu was detected in the grain boundaries showing that Cu containing precipitates were not found in these regions. Point C, in the figure, which is essentially on the eutectic phase, is enriched with elements such as Al, Zn, Mg, Si, and Cu. Among these elements, Si has the highest amount after Al, hence for the likely presence of α phase along with the eutectic phase of $AlCuMgZn$ characteristics. Finally, point D is rich in Mg and Al. It also covers a large area and is indicative of the matrix composition. It is important to mention that Zn and Mg are present in most of the WM places [43].

Figure 13 gives EDS point analyses of three regions in the HAZ. It is important to mention that the low value of Si, shown in the figure, is unreliable. At point A, which is close to the grain boundary, there are 70.53%, 11.52, 9.51, and 4.2% for Al, Fe, Cu, and Zn, respectively. Point B contains elements such as Al, Cu, Zn, and Mg that are sequentially the highest concentrations. This point features a remnant of eutectic phase. The matrix structure of point C contains Al, Zn, and Mg elements. Based on the results of the analysis of different locations of HAZ, Al, Zn, and Mg are mostly present in this region.

3.4 The effect of frequency and current amplitude on the porosity of the weld metal

Another significant phenomenon that is observed during the DP-GMAW process is the reduction of the porosity of the WM. Increasing the agitation or shaking of the weld pool is the primary mechanism for the porosity reduction of the WM [44]. Moreover, based on the findings of Pal and Pal [33, 45], the DP-GMAW process can be very

Fig. 12 SEM micrograph and EDS analyses of the WM showing the composition of different locations in terms of the presence of precipitating alloying elements. **a** SEM micrograph of the WM. **b** EDS analysis of point A. **c** EDS analysis of point B. **d** EDS analysis of point C. **e** EDS analysis of point D



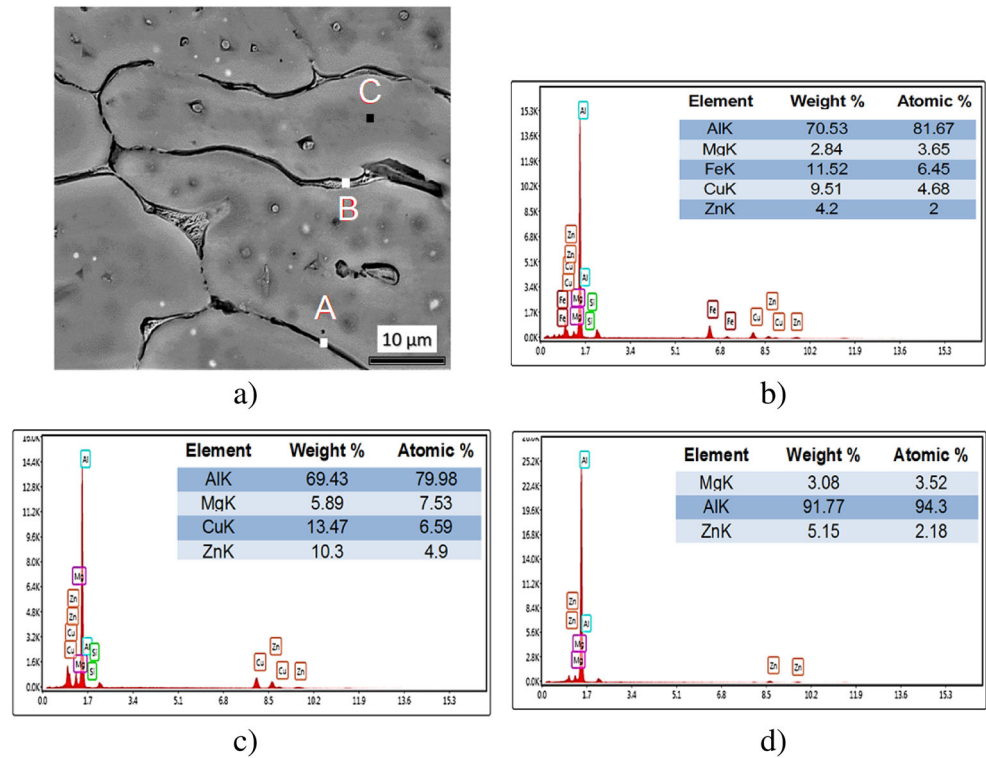
beneficial in reducing the porosity of the WM. Therefore, in this study, the effect of two critical parameters of the DP-GMAW process on the average porosity of the WM was assessed. Figures 14 and 15 show the average porosity of the WM at different amounts of thermal frequency and the current amplitude, respectively. The average diameter values of porosities were measured for each sample, which were 53, 26, and 19 μm for the frequencies of 1, 2, and 3, respectively. Also, these values for the current amplitudes of 9, 27, and 45 A were measured as 55, 40, and 47 μm .

Based on these results, increasing the thermal frequency has led to a substantial reduction in the porosity of the WM. In fact, by increasing the frequency from 1 to 2 Hz, the porosity reduction of the WM was more sensible than increasing the frequency from 2 to 3 Hz. It is important to mention that hydrogen bubbles were the primary source of the porosity in the WM. Therefore, a significant

amount of hydrogen bubbles found an opportunity to exit from the pool by increasing the frequency and subsequently by maximization of the agitation of the weld pool, thus for the lower amount of trapped porosity in the WM. The findings of this study are well-matched with the results reported by Wang and Xue [24].

Current amplitude, as another crucial parameter of the process, affects the amount of porosity in the WM. Since the agitation created under the condition of increasing the current amplitude was more than the turmoil created by increasing the thermal frequency, the reduction in the average porosity under this circumstance was more pronounced. Based on the results obtained in this study, the current amplitude of 27 A provides the lowest level of porosity in the WM. In a sense, increasing the current amplitude was more beneficial in reducing the porosity of the WM compared with increasing the thermal

Fig. 13 SEM micrograph and EDS results for the chemical composition analysis of the HAZ zone of S1 sample. **a** SEM micrograph of the HAZ zone. **b** EDS analysis of point A. **c** EDS analysis of point B. **d** EDS analysis of point C



frequency. On the other hand, a further increase in current amplitude from the value of 27 A results in an increase in the amount of porosity in WM. This is due to the fact that, as discussed earlier, the cooling rate increases by increasing the current amplitude. Therefore, there would be less time available for the gas bubbles to escape from the weld pool. Using the average diameter of the porosities and their numbers, the average area of the porosities was calculated for each sample. Results showed that the trend of

changing the area of the porosities is well-matched with the trend of number variation.

3.5 Mechanical properties

In terms of the mechanical properties, the effect of changing thermal frequency and current amplitude of the DP-GMAW process was studied on changing the hardness of the WM, HAZ, and BM. Figures 16 and 17 show the effect of thermal frequency and current amplitude on the hardness variation of the weldment of AA7075, respectively. Also, Table 4 gives

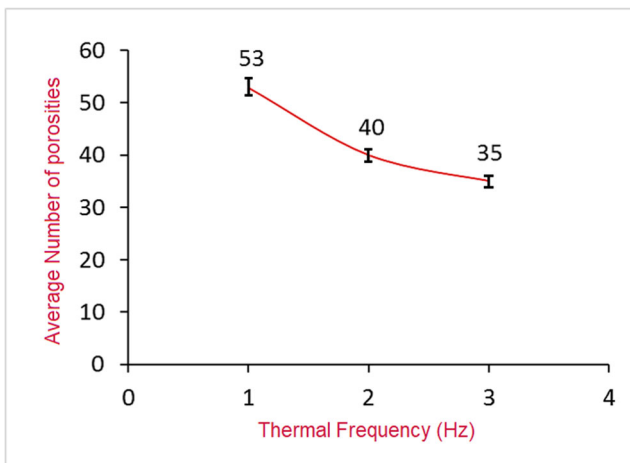


Fig. 14 The effect of thermal frequency of the DP-GMAW process on the porosity of the WM

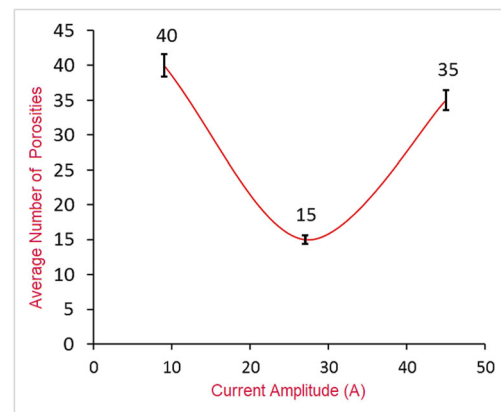


Fig. 15 The effect of the current amplitude of the DP-GMAW process on the porosity of the WM

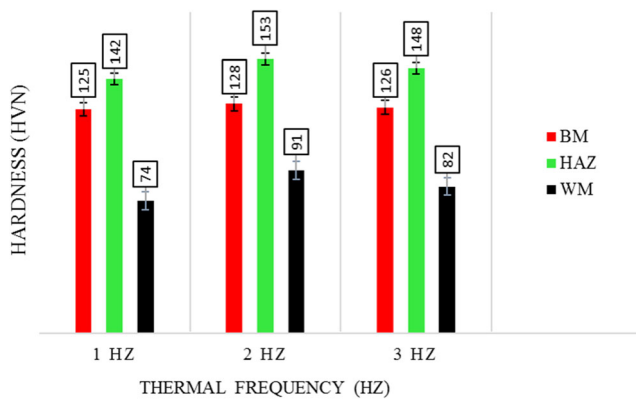


Fig. 16 Hardness variation of the weldment of the AA7075 alloy under different thermal frequencies

the hardness variation of the weldment at different thermal frequency and current amplitude.

The results of the hardness test indicate that hardness decreases by moving from the BM towards the WM. The first mechanism to propose for such a decrease in the hardness of the WM is the grain growth in this region. Based on the Hall-Petch equation ($\sigma = \sigma_i + \frac{k}{\sqrt{D}}$), such a reduction is not uncommon. Moreover, the filler metal used for the AA7075 joints was an AlMg₅-type alloy. Therefore, the existence of this difference in the chemical composition makes it impossible for the filler metal to provide the required alloying elements to match with that of the AA7075 composition [46]. As well, part of the alloying elements vaporizes during the welding process. In other words, it is the reason for the reduction in the hardness of the melted region of this alloy [47]. They showed that the segregation of alloying elements such as Zn, Mg, and Cu in the grain boundaries, during the melting and solidification process, is the leading cause of such a reduction in hardness.

Based on Fig. 16, the HAZ has higher hardness compared with the BM. About 13% increment in hardness was observed

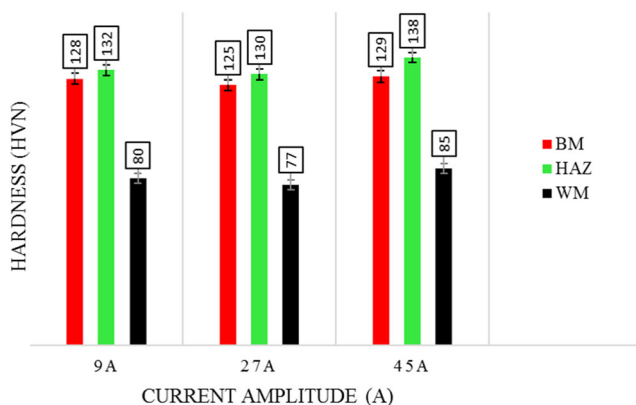


Fig. 17 Hardness variation of the weldment of the AA7075 alloy under different current amplitudes

in this region. Also, under the thermal frequency of 2 Hz, the highest amount of hardness was obtained in the WM. The hardness increment of the HAZ can be explained by the formation of very fine grains due to the recrystallization phenomenon occurring under the influence of welding sequences. The results of this study were in accordance with the results of Wang et al. [19]. As well, the results are also matched with the findings of Ishak et al. [43]. The average grain size in the HAZ region was even lower than the grain size in the BM. Also, in assessing the effectiveness of the current amplitude on the hardness of the weldment in Fig. 17, the highest amount of hardness was obtained in the HAZ region. Moreover, the highest amounts of hardness for the HAZ and the WM were obtained under the current amplitude of 45 A. In that sense, about 8% increase in hardness was obtained in these two regions compared with the BM.

4 Conclusions

The following conclusions were drawn by studying the effect of the DP-GMAW process parameters during the welding of AA7075 alloy. The parameters included thermal frequency and current amplitude. Their impact on the weldability, microstructural evolution, and mechanical properties were investigated. The following conclusions were drawn:

1. Results showed that the variation of thermal frequency leads to the variation of the fusion line. In that sense, an increase in the thermal frequency led to the closeness of the ripples in the weld metal and reduced the distance between the peaks.
2. The microstructure of the partially melted zone (PMZ) showed a coarse columnar structure which was located between the WM and the HAZ regions. Increasing the frequency from 1 to 3 Hz and also increasing the current amplitude from 9 to 45 A significantly reduced the length of the PMZ.
3. During the DP-GMAW process, cracking was not observed in the joint area at thermal frequencies of 1, 2, and 3 Hz, and current amplitude of 9, 27, and 45 A. This was ascribed to the substantial reduction of grain size in this region. Results showed that there is an optimal value of 2 Hz for the thermal frequency, and 45 A for the current amplitude to obtain the finest grain size.
4. Increasing thermal frequency and current amplitude reduced the porosity of the WM. Among these parameters, the current amplitude was more effective in reducing the porosity of the WM. It was found that there is an optimum value of the current amplitude to achieve minimum

Table 4 Hardness variation (HVN) of the weldment

Position	Thermal frequency (Hz)			Current amplitude (A)		
	1	2	3	9	27	45
Weld metal (WM)	74	91	82	80	77	85
Heat-affected zone (HAZ)	142	153	148	132	130	138
Base metal (BM)	171			171		

porosity. A further increase in current amplitude from this optimum value led to a rise in the amount of porosity.

- Results showed that, compared with the BM, about 13% increment in hardness was achievable in the HAZ. On the other hand, the highest amount of hardness in the WM was obtained under the thermal frequency of 2 Hz.
- Increasing the current amplitude increased the hardness of the WM. The highest hardness values for the HAZ and the WM were obtained under the current amplitude of 45 A. In that regard, compared with the BM, about 8% increase in hardness was obtained in the HAZ and the WM regions.

Author contribution Behnam Soltani: Experimentation, data collection, and original draft preparation.

Amirreza Farnia: Methodology, writing, reviewing, and supervision.

Seyed Hashem Mousavi Anijdan: Writing, reviewing, and supervision.

Data availability The raw/processed data required to reproduce these findings cannot be shared at this time as the data also forms part of an ongoing study.

Declarations

Consent to participate The authors declare their consent to participate in this article and ensure the author group, the corresponding author, and the order of authors are all correct at submission.

Consent to publish The authors declare their consent to publish this article in “The International Journal of Advanced Manufacturing Technology.”

Competing interests The authors declare no competing interests.

Ethical approval Not applicable. The authors have no relevant financial or non-financial interests to disclose.

References

- Oliveira JP, Crispim B, Zeng Z, Omori T, Braz Fernandes FM, Miranda RM (2019) Microstructure and mechanical properties of gas tungsten arc welded Cu-Al-Mn shape memory alloy rods. *J Mater Process Technol* 271:93–100
- Zhang Y, Zuo TT, Tang Z, Gao MC, Dahmen KA, Liaw PK, Lu ZP (2014) Microstructures and properties of high-entropy alloys. *Prog Mater Sci* 61:1–93
- Oliveira JP, Curado TM, Zeng Z, Lopes JG, Rossinyol E, Park JM, Schell N, Braz Fernandes FM, Kim HS (2020) Gas tungsten arc welding of as-rolled CrMnFeCoNi high entropy alloy. *Mater Des* 189:108505
- Dursun T, Soutis C (2014) Recent developments in advanced aircraft aluminum alloys. *Mater Des* 56:862–871
- Williams JC, Starke EA (2003) Progress in structural materials for aerospace systems. *Acta Mater* 51:5775–5799
- Lippold, John C., Kiser, Samuel, D., DuPont, John N., 2009. *Welding metallurgy and weldability of nickel-base alloys*, ISBN 978-0-470-08714-5, Wiley.
- Lippold, John C., Kotecki, Damian J. (2005) *Welding metallurgy and weldability of stainless steels*, ISBN: 978-0-471-47379-4, Wiley.
- Forghani M (2018) Effect of PWHT variables on microstructure and mechanical properties of the Al-Zn weld metal. *J Environ Friendly Mater* 2018(2):19–22
- Mishra RS, Ma ZY (2005) Friction stir welding and processing. *Mater Sci Eng R* 50:1–78
- Squillace A, Fanzo AD, Giorleo G, Bellucci F (2004) A comparison between FSW and TIG welding techniques: modifications of microstructure and pitting corrosion resistance in AA 2024-T3 butt joints. *J Mater Process Technol* 152:97–105
- Nie Z (2016) Experimental study and modeling of H13 steel deposition using laser hot-wire additive manufacturing. *J Mater Process Technol* 235:171–186
- Temmar M, Hadji M, Sahraoui T (2011) Effect of post-weld aging treatment on mechanical properties of tungsten inert gas welded low thickness 7075 aluminium alloy joints. *Mater Des* 32:3532–3536
- Halzer M, Hofmann K, Mann V, Hugger F, Roth S, Schmidt M (2016) Change of hot cracking susceptibility in welding of high strength aluminum alloy AA7075. *Phys Procedia* 83:463–471
- Balasubramanian V, Ravisankar V, Reddy GM (2008) Effect of pulsed current welding on mechanical properties of high strength aluminum alloy, *Int J. Adv Manuf Technol* 36:254–262
- Balasubramanian V, Ravisankar V, Reddy GM (2008) Effect of postweld aging treatment on fatigue behavior of pulsed current welded AA7075 aluminum alloy joints. *J Mater Eng* 17:224–233
- Yi J, Cao SF, Li LX, Guo PC, Liu KY (2015) Effect of welding current on morphology and microstructure of Al alloy T-joint in double-pulsed MIG welding. *Trans Nonferrous Metals Soc China* 25:3204–3211
- Da Silva CLM, Scotti A (2004) Performance assessment of the (Trans) Vrestraint tests for determining solidification cracking susceptibility when using welding processes with filler metal. *Meas Sci Technol* 15:2215
- Liu AH, Tang XH, Lu FG (2013) Arc profile characteristics of Al alloy in double-pulsed GMAW. *Int J Adv Manuf Technol* 65:1–7

19. Wang LL, Wei HL, Xue JX, DebRoy T (2018) Special features of double pulsed gas metal arc welding. *J Mater Process Technol* 251:396–375
20. Mendes da Silva CL, Scotti A (2006) The influence of double pulse on porosity formation in aluminum GMAW. *J Mater Process Technol* 171:366–372
21. Yao P, Xue J, Meng W, Zhu S (2009) Influence of processing parameters on weld forming in double-pulse MIG welding of aluminum alloy. *Trans China Weld Inst* 30:69–72
22. Nakata K, Matsuda F, Jogan S, Harada S, Ueyama T (1994) Improvement of weld solidification crack susceptibility of Al-Zn-Mg ternary alloy by low-frequency pulsed GMA (MIG) welding with trial-manufactured Zr-added Al-high-Mg welding wire. *Weld Int* 8:690–696
23. Yamamoto, H., Harada, S., Ueyama, T., Ogawa, S., Matsuda, F., 1993. Nakata, K. Beneficial effects of low-frequency pulsed MIG welding on grain refinement of weld metal and improvement of solidification crack susceptibility of aluminium alloys: Study of low-frequency pulsed MIG welding. *Weld Int*, 7, 456–461.
24. Wang L, Xue J (2017) Perspective on double pulsed gas metal arc welding. *Appl Sci* 7:894
25. Wang Z, Oliveira JP, Zeng Z, Bu X, Peng B, Shao X (2019) Laser beam oscillating welding of 5A06 aluminum alloys: microstructure, porosity and mechanical properties. *Opt Laser Technol* 111:58–65
26. Sun J, Nie P, Feng K, Li Z, Guo B, Jiang E (2017) The elimination of pores in laser welds of AISI 304 plate using different shielding gases. *J Mater Process Technol* 248:56–63
27. Zhan X, Gao Q, Gu C, Sun W, Chen J, Wei Y (2017) The porosity formation mechanism in the laser-MIG hybrid welded joint of Invar alloy. *Opt Laser Technol* 95:86–93
28. Berger P, Hugel H, Graf T (2011) Understanding pore formation in laser beam welding. *Phys. Procedia* 12:241–247
29. Wang L, Gao M, Zhang C, Zeng X (2016) Effect of beam oscillating pattern on weld characterization of laser welding of AA6061-T6 aluminum ally. *Mater Des* 108:707–717
30. Ke W, Bu X, Oliveira JP, Xu W, Wang Z, Zeng Z (2021) Modeling and numerical study of keyhole-induced porosity formation in laser beam oscillating welding of 5A06 aluminum alloy. *Opt Laser Technol* 133:106540
31. Guo W, Wan Z, Peng P, Jia Q, Zou G, Peng Y (2018) Microstructure and mechanical properties of fiber laser welded QP980 steel. *J Mater Process Technol* 256:229–238
32. Metals Handbook, Vol.2, 1990. Properties and selection: nonferrous alloys and special-purpose materials, ASM International 10th Ed.
33. Kou S (2002) *Welding metallurgy*, 2nd edn. University of Wisconsin, USA
34. Pal K, Pal SK (2010) Effect of pulse parameters on weld quality in pulsed gas metal arc welding: a review. *J Mater Eng Perform* 20:918–931
35. Goyal V, Ghosh P, Saini J (2008) Influence of pulse parameters on characteristics of bead-on-plate weld deposits of aluminum and its alloy in the pulsed gas metal arc welding process. *Metall Mater Trans A* 39:3260–3275
36. Engler O, Hirsch J (2002) Texture control by thermomechanical processing of AA6xxx Al-Mg-Si sheet alloys for automotive applications—a review. *Mater Sci Eng A* 336:249–262
37. Jin L, Xue J, Zhang Z, Hu Y (2018) Effects of thermal frequency on microstructures, mechanical and corrosion properties of AA6061 joints. *Appl Sci* 8:540
38. Peng D, Shen J, Tang Q, Wu CP, Zhou YB (2013) Effects of aging treatment and heat input on the microstructures and mechanical properties of TIG-welded 6061-T6 alloy joints. *Int J Miner Metall Mater* 20(3):259–265
39. Wang L, Jin L, Huang W, Xu M, Xue J (2016) Effect of thermal frequency on AA6061 aluminum alloy double pulsed gas metal arc welding. *Mater Manuf Process* 31:2152–2157
40. Rokhlin SI, Guu AC (1993) A study of arc force, pool depression and weld penetration during gas tungsten arc welding. *Weld J* 72(8):381–390
41. Wang L (2017) Pathway to microstructural refinement through double pulsed gas metal arc welding. *Scr Mater* 134:61–65
42. Kimura R, Hatayama H, Shinozaki K, Murashima I, Asada J, Yoshida M (2009) Effect of grain refiner and grain size on the susceptibility of Al-Mg die casting alloy to cracking during solidification. *J Mater Process Technol* 209:210–219
43. Ishak M, Salleh MNM, Aisha SR (2017) The mechanical and microstructural study of welded AA7075 using different filler metals. *International Journal of Computational Methods and Experimental Measurements (CMEM)* 5:696–712
44. Kumagai M (2003) Recent technological developments in welding of aluminium and its alloys. *Weld Int* 17:173–181
45. Pal K, Pal SK (2010) Study of weld joint strength using sensor signals for various torch angles in pulsed MIG welding. *J Manuf Sci Technol* 3:55–65
46. Alatorre N, Ambriz RR, Noureddine B, Amrouche A, Talha A, Jaramillo D (2014) Tensile Properties and fusion zone hardening for GMAW and MIEA welds of a 7075-T651 aluminum alloy. *Acta Metall Sin (Engl Lett)* 27:694–704
47. Zhang L, Li X, Nie Z, Huang H, Sun J (2016) Softening behavior of a new Al-Zn-Mg-Cu alloy due to TIG welding. *J Mater Eng* 25:1870–1879

Publisher's note Springer Nature remains neutral with regard to jurisdictional claims in published maps and institutional affiliations.